Characterizing Individual Scattering Events by Measuring the Amplitude and Phase of the Electric Field Diffusing through a Random Medium

Zhongping Jian, Jeremy Pearce, and Daniel M. Mittleman

Department of Electrical and Computer Engineering, Rice University, MS 366, Houston, Texas 77251-1892, USA

(Received 24 March 2003; published 18 July 2003)

We describe observations of the amplitude and phase of an electric field diffusing through a three-dimensional random medium, using terahertz time-domain spectroscopy. These measurements are spatially resolved with a resolution smaller than the speckle spot size and temporally resolved with a resolution better than one optical cycle. By computing correlation functions between fields measured at different positions and with different temporal delays, it is possible to obtain information about individual scattering events experienced by the diffusing field. This represents a new method for characterizing a multiply scattered wave.

DOI: 10.1103/PhysRevLett.91.033903 PACS numbers: 42.25.Dd, 02.50.–r, 78.47.+p

Measurements of diffuse photons have proved to be a powerful tool in statistical optics. Narrow-band diffuse photon density waves can be used for the imaging of objects immersed in a random medium [1–4]. It is also possible to extract information using diffusing wave spectroscopy, which involves measurements of the temporal intensity or field correlations in a dynamic random medium [5–7]. Alternatively, one can obtain similar data from spatial correlations within a speckle pattern [8–10]. All of these techniques have found broad applicability, particularly in the field of biomedical imaging. However, due to the difficulties associated with determining the phase of an optical field, all rely on measurements of light intensity, rather than electric field. Even in the case of low-coherence interferometry, one does not obtain a measurement of the optical phase, but only of the local variations of the path-length resolved reflectance [11–14]. Furthermore, intensities are generally measured only in an average sense, over a time scale much longer than the optical period. Time-resolved field measurements of diffusive waves have been performed using microwave techniques [15–17], but these have generally employed a waveguide geometry in which the issue of imaging of buried objects has not often been considered.

Here, we demonstrate a direct measurement of the diffusing electric field in a random medium, with high temporal resolution. This measurement permits us to obtain information about the locations of *individual scattering events* experienced by portions of the diffusing field. This information is typically not experimentally accessible because the measured field generally consists of a superposition of many random phasors, corresponding to waves that have traversed many different possible paths [18]. However, by computing the temporal correlations between waves measured at different spatial locations, we are able to highlight the portions which originate from a single scattering event. This represents a completely new method for characterizing a random medium, since the concept of locating individual scattering events within a diffusing wave has not previously been considered. We note that it has recently become possible to measure the amplitude and phase of ultrashort optical pulses [19], so our results could in principle be extended to biologically relevant wavelengths in the near infrared. Thus, these measurements open up new possibilities for imaging in biological media.

Our experimental technique is based on terahertz time-domain spectroscopy (THz-TDS). To simulate a random medium, we use a large number of Teflon spheres, with diameter 0.794 ± 0.025 mm. Teflon is an excellent material for these measurements, because of its low absorption and dispersion in the THz range [20]. The spheres are poured into a cylindrical Teflon cell with internal radius of 2.3 cm. The volume fraction of the spheres in the sample cell is 0.56 ± 0.04. The single-cycle pulses of terahertz radiation are generated and detected using ultrafast photoconductive antennas [21]. Previously, we have used THz-TDS to measure the optical mean free path in these samples in the spectral range 0.1–1 THz, by observing the decay of the ballistic transmission [22]. The transmitter is fixed, but the receiver antenna is mounted at the end of a rail which pivots around the central axis of the cylindrical sample cell, as shown in Fig. 1. The field emerging from the random medium can thus be easily measured at many different spatial locations [23]. For each fixed configuration of the random medium, we measured waveforms at angles of $\theta = 65°, 66°, \ldots, 75°$ and $\theta = 105°, 106°, \ldots, 115°$, corresponding to forward and backward scattering, respectively. Typical input and scattered waveforms are shown in Fig. 2.

For a given random configuration, we expect that the correlation between fields measured at two different angles, $\langle E_{\theta_1}(t) E_{\theta_2}(t) \rangle$, decreases with increasing $\delta\theta \equiv \theta_2 - \theta_1$ [18]. Since we directly measure $E(t)$, we may easily compute this correlation coefficient, averaged

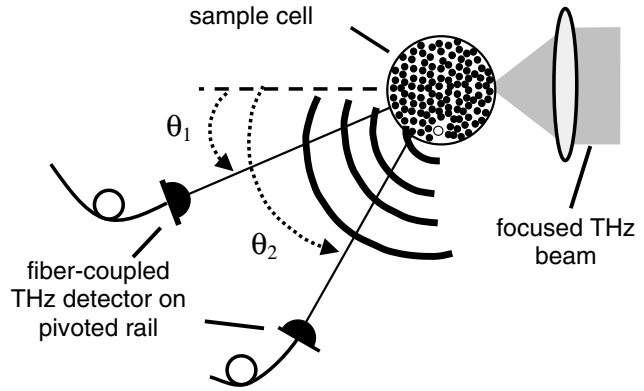

FIG. 1. Schematic of the experimental setup, showing the fiber-coupled THz detector in two different positions (labeled θ_1 and θ_2). A spherical wave produced by a hypothetical scattering event, centered to the right of the axes of both of the displayed detector locations, is also shown. This partial spherical wave produces a correlated signal at the two detectors, with a temporal shift resulting from the geometrical path length difference. The detector at θ_2 receives the signal earlier.

over all configurations for each value of $\delta\theta$. The result shows an exponential decay, with an angular $1/e$ width of $\sim 3.7°$. This is essentially a measure of the mean size of a speckle spot, which is related to the illuminated area on the sample cell input facet [8,24].

A more surprising result can be found by computing the correlation function between portions of the measured time-domain waveforms, rather than using the entire waveform. By choosing a temporal window, one can highlight correlations that occur at particular time delays. For example, we expect that the later parts of a particular pair of wave forms show smaller correlations than the earlier parts, since these late-arriving parts have scattered more times [25]. In addition, partial waves may arrive at each detector location with a different delay (see Fig. 1), so correlated signals may appear at nonzero values of the correlation offset. To formalize the computational procedure, we define a correlation function with a variable-delay window:

$$C_{\delta\theta}(\tau, T) = \frac{1}{C_0}\langle [E_{\theta_1}(t) \cdot W_T(t)][E_{\theta_2}(t+\tau) \cdot W_T(t+\tau)]\rangle,$$

where τ is the correlation offset. $W_T(t)$ is a window function centered at $t = T$. It is defined to be unity in a symmetric window about $t = T$ and zero otherwise. The window width is fixed at 50 ps, approximately equal to the inverse coherence bandwidth for our experimental geometry [26]. As usual, the angular brackets indicate integration with respect to t, followed by an ensemble average over all waveform pairs with the specified value of $\delta\theta$. C_0 is a normalization factor which ensures that $C_{\delta\theta=0}(\tau = 0, T) = 1$. This windowed correlation function is similar to the one recently used for the analysis of coda waves in seismic tomography [25].

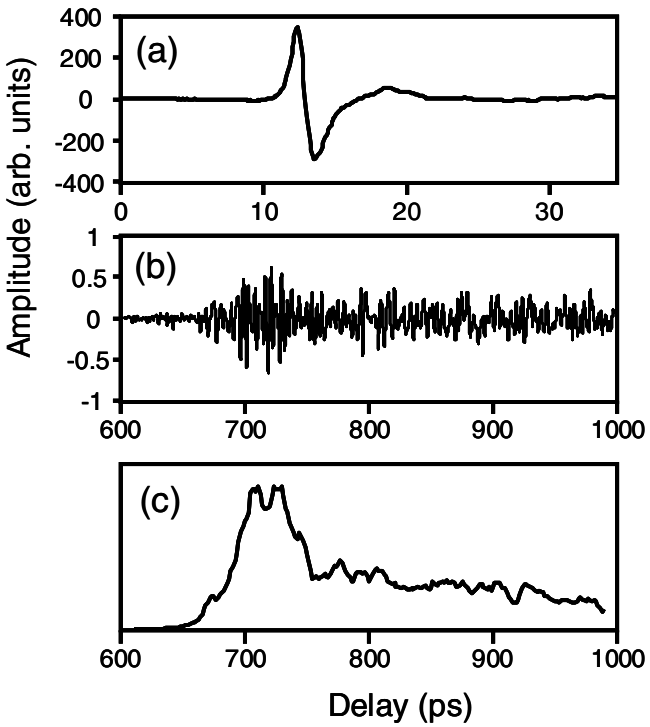

FIG. 2. (a) A typical input waveform. (b) A typical multiply scattered waveform. These data have been spectrally filtered to remove noise at both low and high frequencies. In these data, the zero of the time axis is determined by the length of the optical delay line, and is therefore arbitrary with respect to the arrival of the incident pulse at the input facet of the random medium. However, this arbitrary $t = 0$ is fixed for all measurements. (c) Photon time-of-flight distribution, obtained by averaging the squares of all measured waveforms. This is plotted on the same delay axis as in (b).

A typical result for $C_{\delta\theta}(\tau, T)$ is shown in Fig. 3, for three different values of $\delta\theta$. Clearly, the correlation at zero offset ($\tau = 0$) decreases with increasing window delay T, as a result of the increasing average number of scattering events. Also as expected, the correlation between pairs of waveforms with $\delta\theta = 8°$ is nearly zero, since this is more than twice the angular speckle decay width. However, a strong oscillatory signal, indicating a correlation extending over several cycles of the field, is observed at a window delay of $T \sim 730$ ps. This extended correlation is observed at this value of T for many angular separations, even those which are larger than the angular width of a typical speckle spot. This surprising feature arises when a partial wave from *one particular scattering event gives* rise to synchronized (though not simultaneous) signals at all detector locations. In the example shown here, only one scattering event is observed. However, for other configurations of the random medium, we generally observe numerous oscillatory signatures, occurring at various values of T.

From $C_{\delta\theta}(\tau, T)$, it should be possible to determine the location of the particular scattering event which gives rise to the observed correlation. Here, we use the evolution of

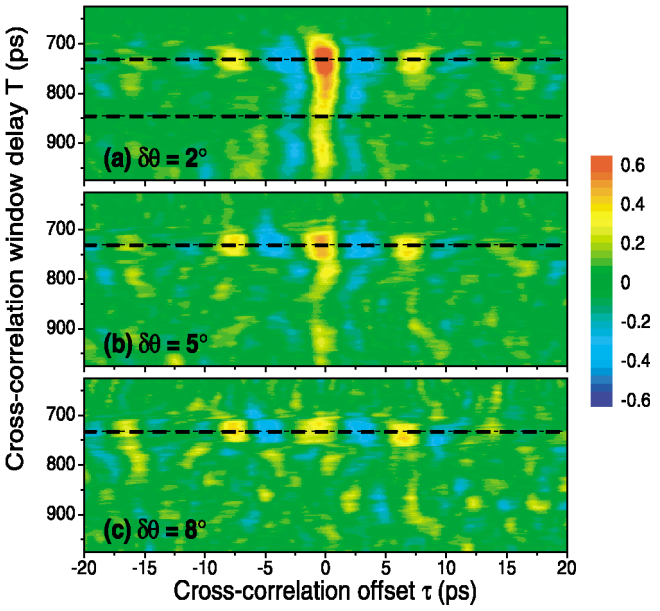

FIG. 3 (color). Correlation function $C_{\delta\theta}(\tau, T)$, plotted versus the correlation offset τ and the delay of the temporal window T. The T axes (vertical axes) are the same as the time axes in Figs. 2(b) and 2(c). These data represent an ensemble average of all pairs of measured fields with the indicated angular separation for one particular realization of the random configuration of scatterers. In this example, an extended oscillatory correlation is observed at a window delay of $T \sim 730$ ps. This correlation persists even for large angular separations. The dashed lines indicate cuts through these data sets displayed in Fig. 4.

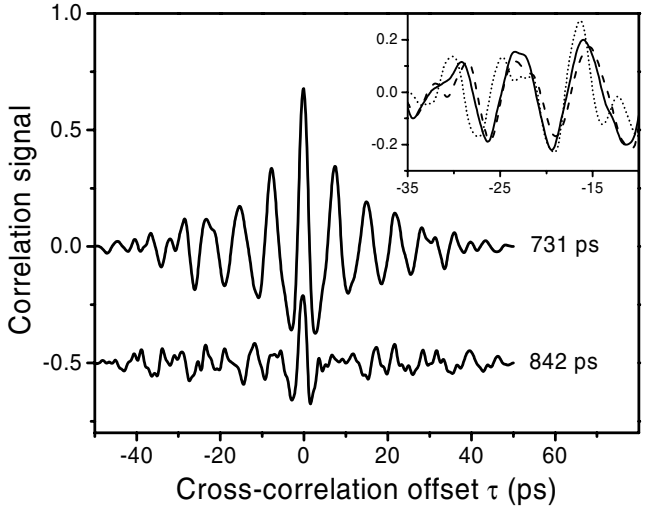

FIG. 4. Correlation functions $C_{\delta\theta}(\tau, T)$ as a function of the cross-correlation offset at two delays corresponding to the two dashed lines in Fig. 3(a). The upper curve has a pronounced oscillatory correlation which is absent at other delays. The lower curve has been shifted downwards by 0.5 for clarity. The inset shows the evolution of a portion of the oscillatory correlation with increasing angular separation (corresponding to the three dashed lines at $T = 730$ ps in Fig. 3; dashed line: $\delta\theta = 2°$, solid line: $\delta\theta = 5°$, dotted line: $\delta\theta = 8°$). As $\delta\theta$ increases, the correlation signal shifts towards negative offsets. This shift is related to the tilt of the correlated wave front emerging from the random medium as illustrated in Fig. 1.

the phase of the correlation to determine the direction from the detector to the scattering event. As shown in the inset of Fig. 4, this phase evolves in a systematic way with increasing $\delta\theta$. In these data, the oscillations shift to a larger negative correlation offset with increasing $\delta\theta$. This indicates that, for waveforms with larger angular separation, a larger (negative) temporal offset is required to cause the oscillations in one waveform to coincide with those in the other. This offset is a result of the geometrical path-length difference arising from the tilt of the wave front. This increasing *negative* shift with increasing $\delta\theta$ means that the correlated portion of the wave front arrived earlier at detectors with larger values of θ, and therefore the corresponding scattering event took place on the side of the detector axis closer to the sample input facet (as illustrated in Fig. 1). Conversely, an increasing *positive* shift with increasing $\delta\theta$ would be observed if the scattering event took place on the opposite side of the detector axis from the input facet. Thus, the evolution of the correlation phase is a direct indication of the direction of the scattering event relative to the detector axis.

From numerous measurements of the type illustrated in Fig. 3, we can collect statistics on the value of the correlation phase shift. This gives a direct measurement of the degree of asymmetry of the radiation emerging from the random medium. We have measured both forward and backward scattering for four distinct configurations of the random medium. We have computed $C_{\delta\theta}(\tau, T)$ for these eight cases and have tabulated the parameters of the numerous oscillatory correlation signatures in each. In these eight data sets, we have observed a total of 98 such signatures, each corresponding to a unique scattering event. For each of these, we have extracted a numerical value for the phase shift of the oscillatory component, as described above. These 98 results are displayed in Fig. 5, divided according to whether the signal was extracted from the forward or the backward scattering data set.

These histograms represent a compelling illustration of the new information that can be obtained using our approach. We have determined that, in the backward direction, the scattering events are largely symmetric. That is, a detector in this region is equally likely to detect scattering events located to the left and right of the detector axis. This follows from the fact that the mean value of the correlation phase shift is approximately zero (-0.03 ± 0.04 ps/deg). On the other hand, in the forward direction the mean value is negative (-0.10 ± 0.04 ps/deg). This indicates a marked asymmetry, with more scattering events located on the side of the detector closer to the input facet.

In conclusion, we have demonstrated a unique method for characterizing the diffusive radiation emerging from a random medium, involving the measurement of both its amplitude and phase. We have developed a simple computational tool which highlights the correlations

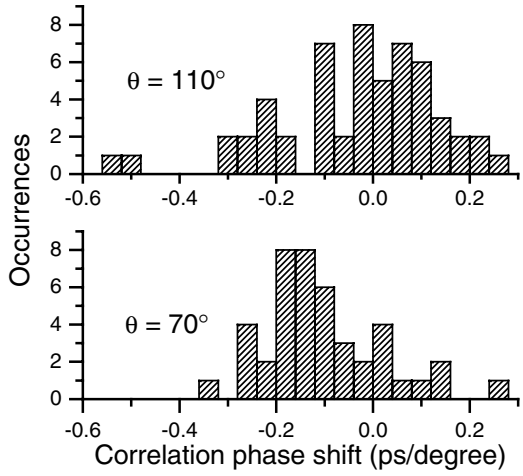

FIG. 5. Histograms of the correlation phase shift, for all of the observed scattering events in measurements of four distinct random configurations. These are displayed for both the cases of forward ($\theta = 65°, \ldots, 75°$) and backward ($\theta = 105°, \ldots, 115°$) scattering. The forward scattering events exhibit an asymmetric correlation phase, indicating that the scattering events are more likely to originate from the side of the detector axis closer to the input beam. In contrast, the backward scattering events are nearly symmetric.

buried within these random waveforms. Using this technique, it is possible to extract information about specific scattering events, which is not possible using conventional measurements. This work should spur further theoretical considerations, since the possibility of time-resolved field measurements has not been considered, other than in a waveguide geometry where imaging considerations are not relevant. Also, we expect that analogous information could be obtained using near-infrared or visible light diffusing through biological tissue. This could in turn lead to a new method for diffuse photon imaging with phase coherent detection.

[1] M. A. O'Leary *et al.*, Opt. Lett. **20**, 426–428 (1995).
[2] D. L. Lasocki, C. L. Matson, and P. J. Collins, Opt. Lett. **23**, 558–560 (1998).
[3] J. Ripoll and M. Nieto-Vesperinas, Opt. Lett. **24**, 796–798 (1999).
[4] J. C. Schotland and V. A. Markel, J. Opt. Soc. Am. A **18**, 2767–2777 (2001).
[5] D. J. Pine *et al.*, Phys. Rev. Lett. **60**, 1134–1137 (1988).
[6] D. A. Boas, L. E. Campbell, and A. G. Yodh, Phys. Rev. Lett. **75**, 1855–1858 (1995).
[7] D. A. Boas and A. G. Yodh, J. Opt. Soc. Am. A **14**, 192–215 (1997).
[8] R. Berkovits and S. Feng, Phys. Rev. Lett. **65**, 3120–3123 (1990).
[9] P. Naulleau *et al.*, Opt. Lett. **20**, 498–500 (1995).
[10] C. A. Thompson, K. J. Webb, and A. M. Weiner, J. Opt. Soc. Am. A **14**, 2269–2277 (1997).
[11] Y. Pan *et al.*, Appl. Opt. **34**, 6564–6574 (1995).
[12] G. Popescu and A. Dogariu, Opt. Lett. **24**, 442–444 (1999).
[13] A. Brodsky, S. R. Thurber, and L. W. Burgess, J. Opt. Soc. Am. A **17**, 2024–2033 (2000).
[14] A. L. Petoukhova, W. Steenbergen, and F. F. M. de Mul, Opt. Lett. **26**, 1492–1494 (2001).
[15] A. Z. Genack *et al.*, Phys. Rev. Lett. **82**, 715–718 (1999).
[16] B. A. van Tiggelen *et al.*, Phys. Rev. E **59**, 7166–7172 (1999).
[17] P. Sebbah, R. Pnini, and A. Z. Genack, Phys. Rev. E **62**, 7348–7352 (2000).
[18] J. W. Goodman, *Statistical Optics* (Wiley, New York, 2000).
[19] R. Trebino, *Frequency-Resolved Optical Gating: The Measurement of Ultrashort Laser Pulses* (Kluwer Academic, Boston, 2002).
[20] J. R. Birch, J. D. Dromey, and J. Lesurf, Infrared Phys. **21**, 225–228 (1981).
[21] P. R. Smith, D. H. Auston, and M. C. Nuss, IEEE J. Quantum Electron. **24**, 255–260 (1988).
[22] J. Pearce and D. M. Mittleman, Phys. Med. Bio. **47**, 3823–3830 (2002).
[23] J. V. Rudd, J. L. Johnson, and D. M. Mittleman, Opt. Lett. **25**, 1556–1558 (2000).
[24] M. Tomita and M. Matsuoka, Phys. Rev. B **43**, 13579–13582 (1991).
[25] R. Snieder *et al.*, Science **295**, 2253–2255 (2002).
[26] A. Ishimaru, *Wave Propagation and Scattering in Random Media* (Academic Press, New York, 1978).